Electronic Supplementary Material (ESI) for Nanoscale Advances.

SUPPORTING INFORMATION

Plasmonic Random Laser Enabled Artefact-Free Wide-Field Fluorescence Bioimaging: Uncovering Finer Cellular Features

R. Gayathri[1,2,#], C. S. Suchand Sandeep[1,#], V. S. Gummaluri[1], R. Mohamed Asik[3,4], Parasuraman Padmanabhan[3,5,*], Balázs Gulyás[3,5,6], C. Vijayan[2,*], V. M. Murukeshan[1,*]

[1] Centre for Optical and Laser Engineering (COLE), School of Mechanical and Aerospace Engineering, Nanyang Technological University, 50 Nanyang Avenue, 639798, Singapore
[2] Department of Physics, Indian Institute of Technology Madras, Chennai, 600036, India
[3] Cognitive Neuroimaging Centre (CONIC), Nanyang Technological University, 59 Nanyang Drive, 636921, Singapore
[4] Department of Animal Science, Bharathidasan University, Tiruchirappalli, 620024, India
[5] Lee Kong Chian School of Medicine, Nanyang Technological University, 608232, Singapore
[6] Department of Clinical Neuroscience, Karolinska Institute, 17176 Stockholm, Sweden

[#] These authors contributed equally to this work
[*] Corresponding author email addresses: *ppadmanabhan@ntu.edu.sg*, *cvijayan@iitm.ac.in*, *mmurukeshan@ntu.edu.sg*

S1 Plasmonic random laser and the threshold characteristics

The emission from the plasmonic random laser is collected and the spectrum is analyzed for increasing pump energies. The threshold characteristics such as the emission intensity and the linewidth plotted against the pump fluence are shown in Fig. S1a and b, respectively. The log-log plot of the emission intensity vs excitation fluence shows the typical "S" shaped behavior, characteristic of random lasing. The emission intensity increases rapidly beyond the threshold fluence of 0.116 mJ/cm^2, and the emission linewidth narrows down from 45 nm to 5 nm.

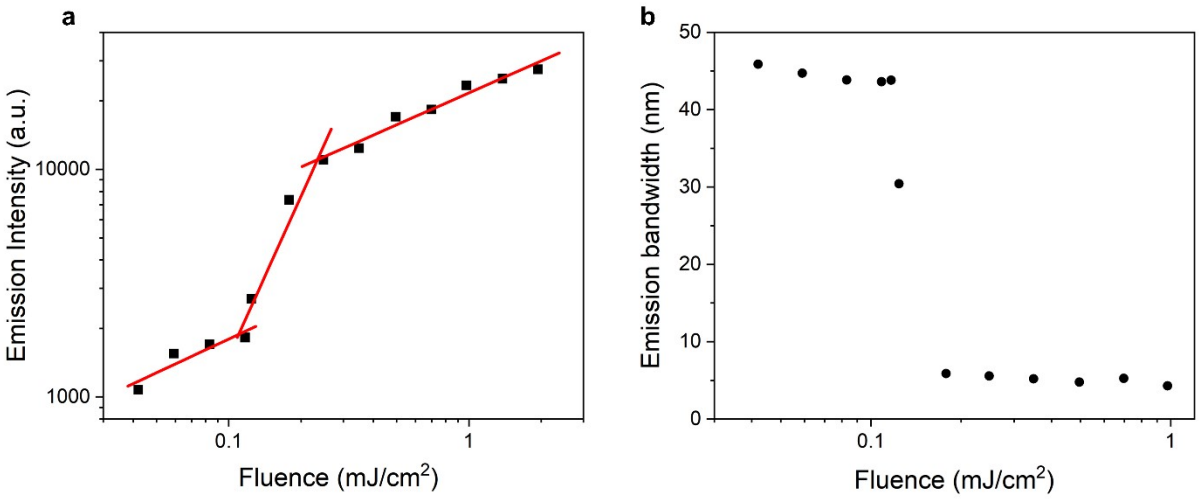

Figure S1. (a) The emission intensity and (b) the line width profile of the random lasing emission with increasing pump fluence.

S2 Imaging of 1951 USAF resolution test chart

The spatial resolution of the system and the image quality offered by different illumination sources are initially evaluated using a 1951 USAF high-resolution test chart (2"× 2" negative target, Edmund Optics). Figure S2a-c shows the image of group 8 and 9 elements of the USAF chart when illuminated with LED, conventional laser and random laser, respectively. The illumination power density used is 450 nW/mm^2 for all the sources. These images are obtained by averaging 15 images, each captured with 0.1 s exposure time. The intensity profile of the group 9 elements over the line marked in red (see Fig. S2a) is shown next to each of the images. The G9E3 (Group 9 Element 3) having a width of 0.78 μm (645.1 lp/mm) is the smallest element in the 1951 high-resolution USAF chart. The vertical and horizontal lines of G9E3 are well resolvable with LED and random laser illumination, suggesting that the resolution of the system is higher than 0.78 μm. However, under conventional laser illumination, these lines are highly distorted and indistinguishable due to the coherent artefacts. This also results in a lower correlation coefficient, 0.56 with conventional laser, compared to 0.89 obtained with both LED and random laser sources.

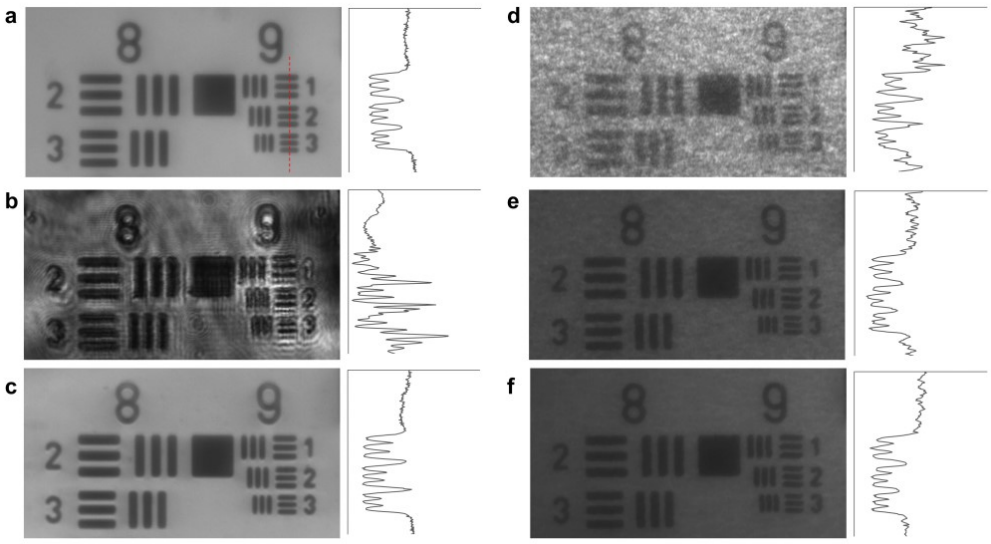

Figure S2. Imaging the 1951 USAF high-resolution test chart to determine the resolution and image quality using different illumination sources. (a) LED. (b) Conventional laser. (c) Random laser. The images (a-c) are obtained by averaging 15 images each captured with 0.1 s exposure time. (d-f), Conventional laser in combination with laser speckle reducer and the images are obtained by averaging 15, 100 and 1000 images respectively, each captured with 0.1 s exposure time. Note that due to the intense coherent artefacts, the intensity of the image captured with the conventional laser (b) is reduced by a factor of 2.5 for better representation, while all the other images are shown as recorded. The intensity profile of the group 9 elements over the line marked in red (a) is shown next to each of the images.

Since the use of dynamic diffuser is one of the state-of-the-art techniques to deal with laser coherence, we also investigated the use of a laser speckle reducer (LSR-3005-12D-VIS,

Optotune) in combination with the conventional laser for illuminating the test chart. The exposure time is set to be 0.1 s. Figure S2d-f shows the images obtained by averaging 15, 100, 1000 images, respectively. To get an image quality and correlation coefficient comparable to that of the random laser, this technique requires a minimum of 1000 images to be averaged (correlation coefficient achieved = 0.75).

S3 Imaging of Siemens star resolution target using laser speckle reducer

The images of a custom-fabricated Siemens star are also captured using the conventional laser in combination with the laser speckle reducer for 0.1 s exposure time. Figure S3a-d shows the images obtained by averaging 1, 10, 100, and 1000 images, respectively. The circular profile at a spatial frequency of 735 lp/mm (spatial resolution of 680 nm) is shown in Fig. S3e. From Fig. S3, it can be seen that the image quality improves with averaging and manages to achieve a correlation coefficient of 0.78 upon averaging 1000 images. However, this value is still less than the value of the correlation coefficient, 0.85, achieved from a single image captured with random laser illumination for 0.1 s. This clearly shows the effectiveness of the random laser in providing high quality artefact-free images with shorter acquisition time, without any post-processing requirements.

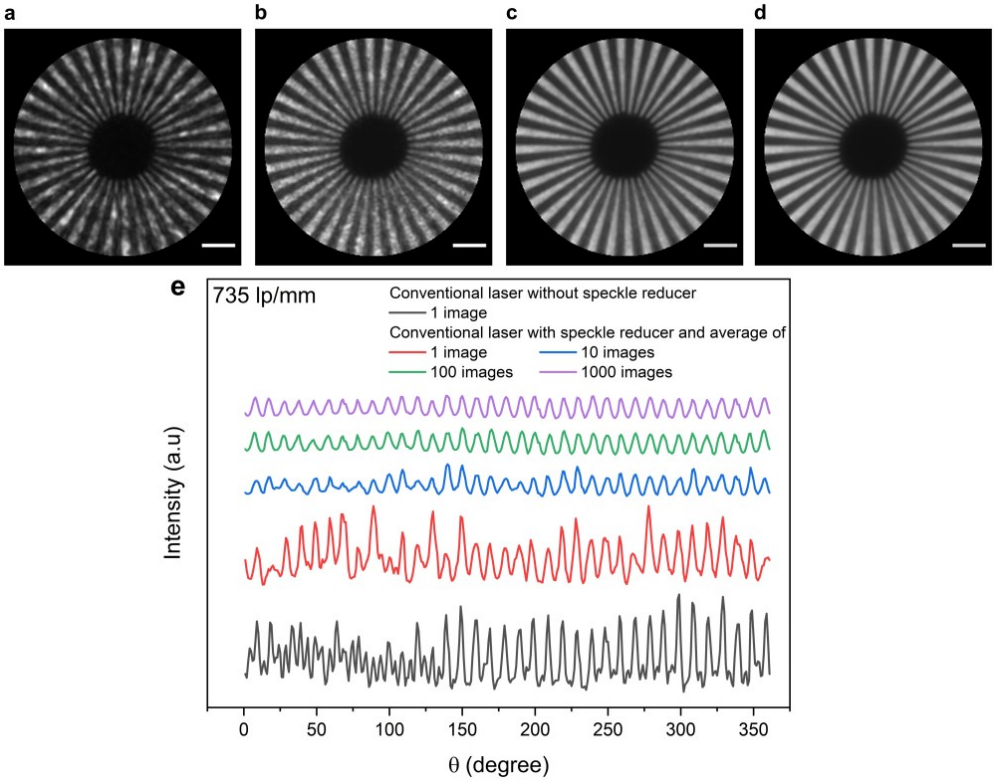

Figure S3. Imaging the Siemens star test target using laser speckle reducer. (a-d) Images obtained by averaging 1, 10, 100 and 1000 images respectively, each captured with 0.1s exposure time. Scale bar is 5 µm. (e) The circular intensity profiles at the spatial frequency of 735 lp/mm. Note that due to the intense coherent artefacts, the intensity of the image (a) is reduced by a factor of 2.5 for better representation, while all the other images are shown as recorded.

S4 Bright-field microscopic imaging of HEK cells

In order to assess the quality offered by the developed system for bright-field bioimaging, the monolayer cell line of human embryonic kidney (HEK293T) is imaged in the trans-illumination mode using the LED, conventional laser and random laser, and the images are shown in Fig. S4a-c, respectively. These images are captured with an exposure time of 0.1 s. Due to the high coherence of conventional lasers, interference fringes and speckles are formed at the imaging plane, making it difficult to obtain bright-field images of the bio-specimen using the conventional laser.

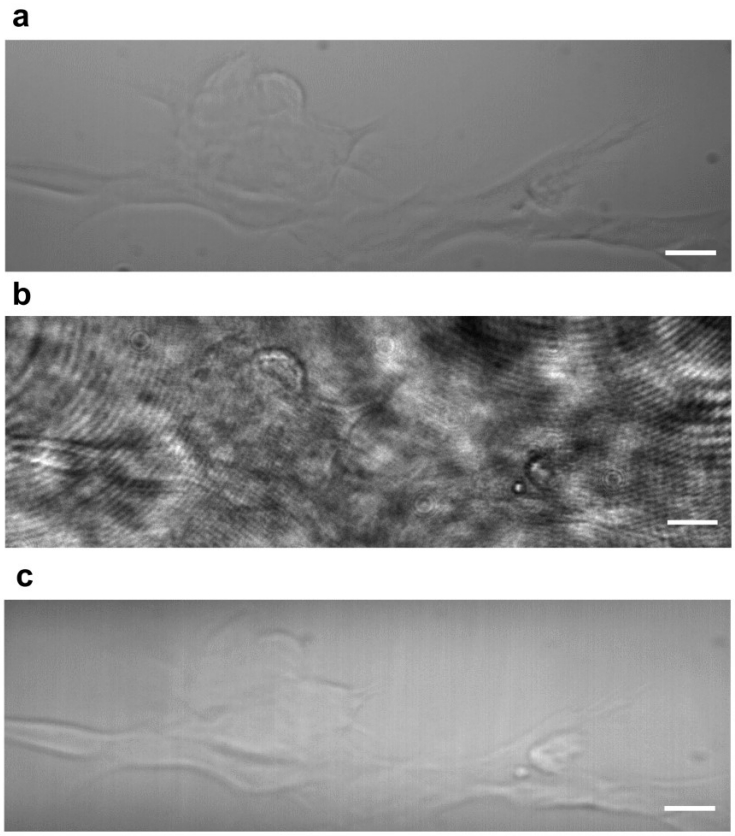

Figure S4. The bright-field microscopic images of monolayer HEK cells captured in the trans-illumination geometry. (a) LED. (b) Conventional laser. (c) Random laser. All the images are captured with 0.1s exposure time. Scale bar is 10 μm.

Laser speckle reducers can be used to reduce the artefacts by averaging over hundreds of images as shown in earlier sections. However, due to the dynamic nature of biological samples and their sensitivity to long-exposure times, it is practically difficult to use laser speckle reducers for bio-imaging. Hence, laser-based fluorescence microscopes usually use an auxiliary broadband source for bright-field imaging, especially to pan through the sample and for focus adjustments. Random laser, being an incoherent laser source, can provide bright-field images with minimal exposure time in addition to the high-quality fluorescence images. This

eliminates the need for switching between the sources for bright-field and fluorescence imaging modes, which is an added advantage for the random laser based fluorescence imaging scheme.

S5 Fluorescence imaging of HEK cells using laser speckle reducer

The fluorescence images of monolayer HEK cells recorded using the conventional laser illumination without and with the laser speckle reducer are shown in Fig. S5a and b, respectively. It can be seen that certain structural details are missing in the image recorded with the conventional laser alone (Fig. S5a). However, these become visible with the use of speckle reducer (Fig. S5b). One such region is highlighted in the red rectangle, and the enlarged view is given below the images. This confirms that coherent artefacts are indeed responsible for the loss of information under conventional laser illumination. It is to be noted that such artefacts in fluorescence images are hard to identify and could potentially lead to misinterpretations.

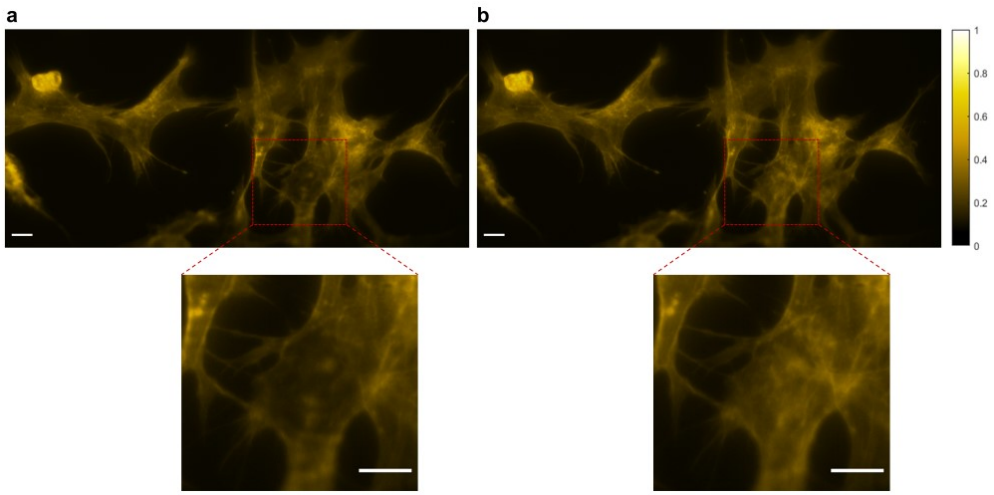

Figure S5. Fluorescence images of HEK cells obtained with illumination using conventional laser combined with laser speckle reducer. (a) Conventional laser alone. (b) Conventional laser with laser speckle reducer. The enlarged view of the region marked in the red box is shown below the corresponding images. Scale bar is 10 μm.

S6 TEM image and XRD pattern of the nanorod scatterer

The transmission electron microscopy (TEM) images of the nanostructures are obtained using JEM 3010 instrument (JEOL, Japan) and the image of a nanorod of length 1.1 μm and diameter 69 nm is shown in Fig. S6a. The X-ray diffraction (XRD) pattern of the synthesised silver nanorod scatterers measured using Cu Kα radiation (λ = 1.54 A°) in powder diffractometer (Panalytical Aeris model) is shown in Fig. S6b. The peaks are indexed in comparison with the JCPDS data (96-150-9147) and it shows that the silver nanostructures have cubic crystal structure. The diameter and length distributions of the nanorods are depicted in Fig. S6c and d, respectively. The average length is estimated to be 0.9 ± 0.4 μm, and the average diameter is 70 ± 9 nm.

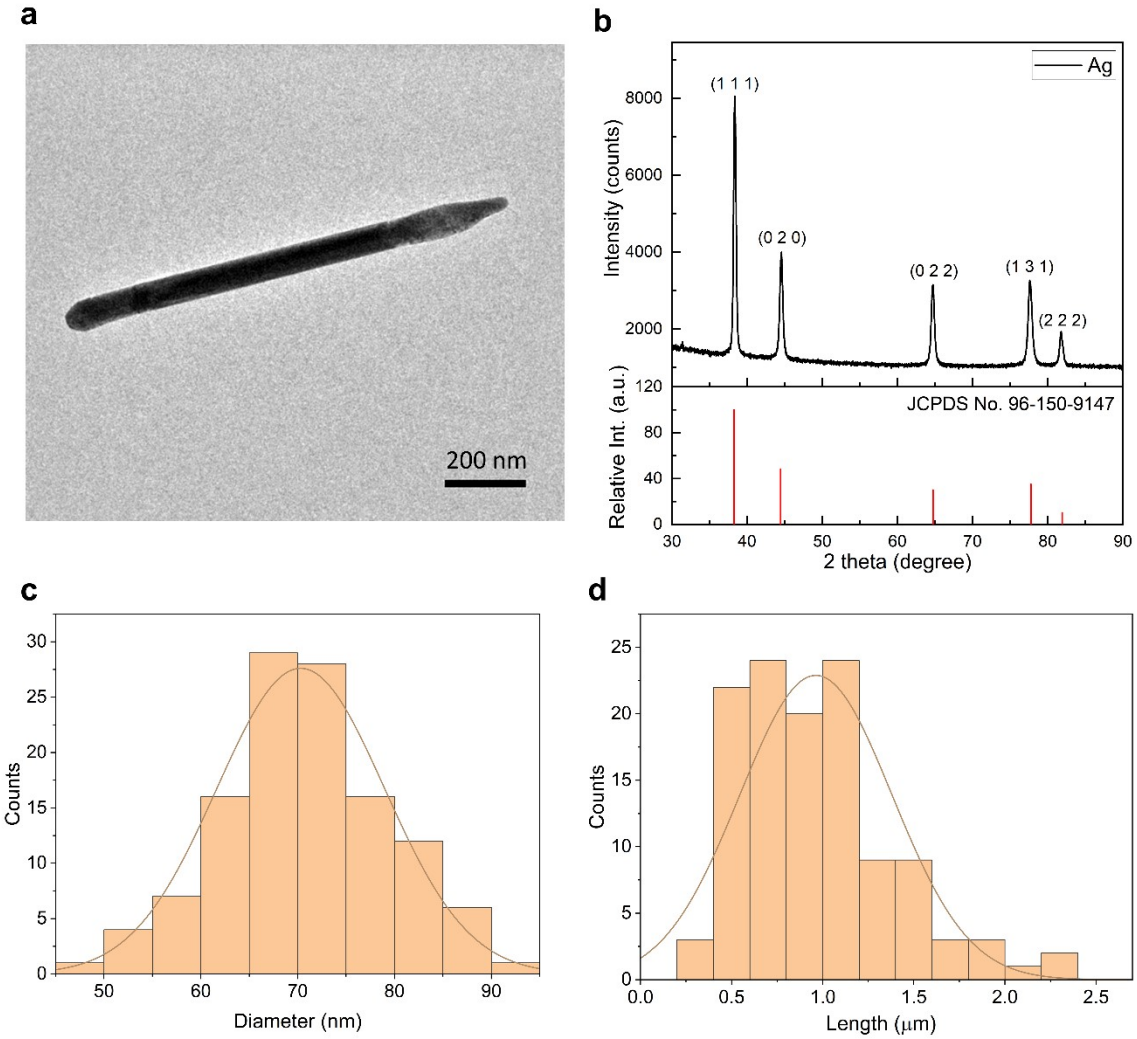

Figure S6. (a) TEM image, (b) X-ray diffraction pattern, and (c-d) size distribution of the synthesized silver nanorod scatterers.

S7 Emission spectra of the illumination sources

The spectra of the three illumination sources recorded at the imaging plane using a fiber optic spectrometer (Avantes, AvaSpec-ULS4096CL-EVO) are shown in Fig. S7.

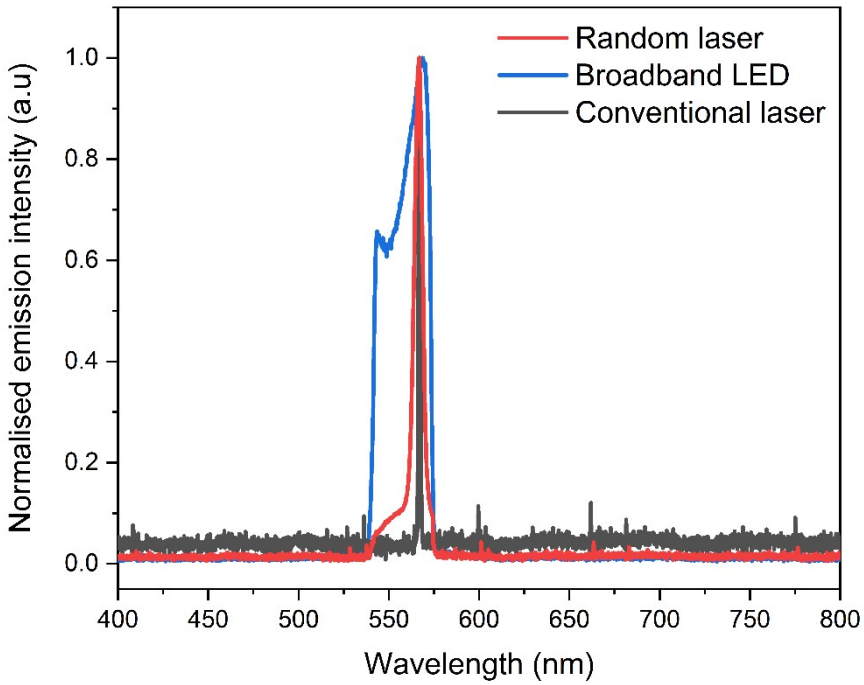

Figure S7. Normalized emission spectra of the three illumination sources used in this work.

S8 LSCM fluorescence image of the HEK sample

The HEK sample stained with Alexa Fluor 568 phalloidin and DAPI is imaged under a commercial laser scanning confocal microscope (LSM800, Zeiss) using 63× oil immersion objective of 1.4 NA and the image recorded is shown in Fig. S8.

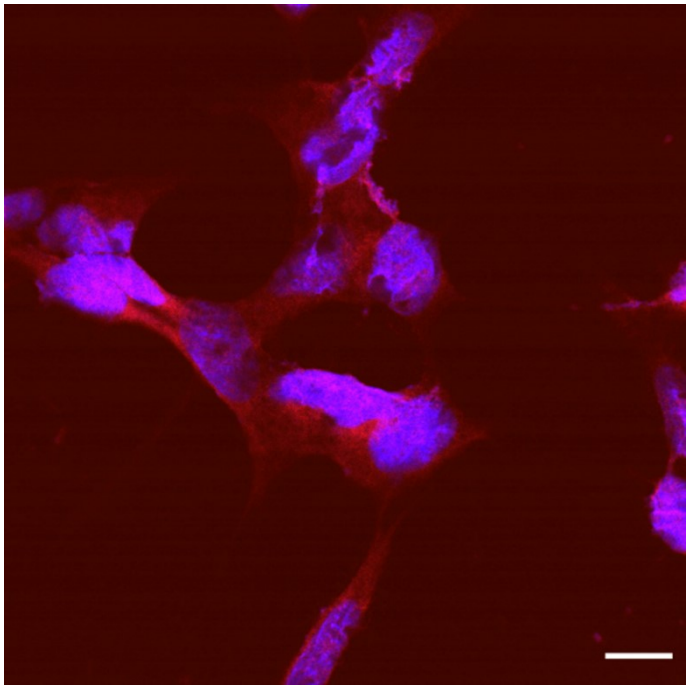

Figure S8. The laser scanning confocal microscopy image of HEK 293T cells stained with Alexa Fluor 568 (red) and DAPI (blue). Scale bar is 10 µm.

Supplementary Visualization 1 (attached separately)

Video file with the fluorescence images of HEK293T cells recorded using random laser and conventional laser illumination shown alternatingly.